A GREEN PLANET VERSUS A DESERT WORLD: ESTIMATING THE MAXIMUM EFFECT OF VEGETATION ON THE LAND SURFACE CLIMATE

AXEL KLEIDON [1]*, KLAUS FRAEDRICH [2] and MARTIN HEIMANN [3]

[1] *Max-Planck-Institut für Meteorologie, Bundesstraße 55, 20146 Hamburg, Germany*
[2] *Meteorologisches Institut der Universität Hamburg, Bundesstraße 55, 20146 Hamburg, Germany*
[3] *Max-Planck-Institut für Biogeochemie, Postfach 10 01 64, 07701 Jena, Germany*

Abstract. We quantify the maximum possible influence of vegetation on the global climate by conducting two extreme climate model simulations: in a first simulation ('desert world'), values representative of a desert are used for the land surface parameters for all non glaciated land regions. At the other extreme, a second simulation is performed ('green planet') in which values are used which are most beneficial for the biosphere's productivity. Land surface evapotranspiration more than triples in the presence of the 'green planet', land precipitation doubles (as a second order effect) and near surface temperatures are lower by as much as 8 K in the seasonal mean resulting from the increase in latent heat flux. The differences can be understood in terms of more absorbed radiation at the surface and increased recycling of water. Most of the increase in net surface radiation originates from less thermal radiative loss and not from increases in solar radiation which would be expected from the albedo change. To illustrate the differences in climatic character and what it would imply for the vegetation type, we use the Köppen climate classification. Both cases lead to similar classifications in the extra tropics and South America indicating that the character of the climate is not substantially altered in these regions. Fundamental changes occur over Africa, South Asia and Australia, where large regions are classified as arid (grassland/desert) climate in the 'desert world' simulation while classified as a forest climate in the 'green planet' simulation as a result of the strong influence of maximum vegetation on the climate. This implies that these regions are especially sensitive to biosphere-atmosphere interaction.

1. Introduction

The terrestrial biosphere and the atmosphere are two interacting subsystems of the Earth. This interaction is accomplished through the strong influence of the biosphere on land surface exchange processes on the one hand, and through the dominant control of climate on the phenology and physiological processes of the biosphere on the other hand. Specifically, vegetation influences the physical appearance and functioning of the land surface in terms of its radiative properties, its hydrological function, and its turbulent characteristics. Vegetation also affects the chemical composition of the atmosphere through its important role for the exchange of atmospheric trace gases such as carbon dioxide, methane and nitrogen

* Corresponding author. Present address: Department of Biological Sciences, Stanford University, Stanford, CA 94305-5020, U.S.A.

Climatic Change **44:** 471–493, 2000.

dioxide (e.g., Schlesinger, 1997). By conducting sensitivity studies with atmospheric General Circulation Models (GCMs), many studies have demonstrated that this biospheric influence on climate is important (see e.g., the recent review by Pielke et al., 1998). For instance, Shukla and Mintz (1982) conducted two extreme simulations with wet and dry land surface conditions respectively (that is, no versus potential evapotranspiration) and reported a considerable effect on surface temperatures, precipitation, and other atmospheric quantities. Noting that vegetation has a large influence on evapotranspiration, they concluded that vegetation plays an important role in the climate system.

On the other hand, climate constrains the activity of the biosphere, mainly through water availability, temperature and radiation. These constraints lead to the general notion that the equilibrium distribution of major vegetation types (biomes) can be understood by climate. This led to the formulation of climate classifications and models of biogeography, such as the ones of Köppen (1923), Holdridge (1947), Budyko (1974), and Prentice et al. (1992). These models have been coupled to climate models in order to investigate the stability of the climate-vegetation system (e.g., Gutman et al., 1984; Henderson-Sellers, 1993; Claussen, 1994; Foley et al., 1996; Claussen, 1998). The coupling is implemented by first associating a set of land surface parameters with each biome, which forms the input for a climate model simulation. The simulated climate then determines the biome distribution, which forms the input for a subsequent climate model simulation. By iterating to an equilibrium between the biome distribution and climate, a two-way interaction between the components is implemented. These studies indicate that the present pattern of biome distribution is uniquely determined by the present-day climate, and thus fairly independent of the initial condition (Claussen, 1998, reports one exception in West Africa where the resulting biome type depends on the initial condition). The great value of this approach is that it stresses the fact that land surface parameters are not independent of each other but mainly represent different aspects of vegetation and that biosphere-atmosphere feedbacks are inherently included.

However, a shortcoming of this approach is that it assumes an equilibrium between vegetation and climate, which may only the case for natural, undisturbed vegetation. Human domination of Earth's ecosystems (e.g., Vitousek et al., 1997), for instance represented by the human use of land, causes a disequilibrium between the two subsystems. The scope of this study is to estimate the maximum range of this disequilibrium, or, in other words, the maximum effect of vegetation on climate. To do so, we conduct a sensitivity study with a state-of-the-art climate model in respect to vegetation, treated as an integrated entity. We first describe the presence of vegetation by its successional stage (Odum, 1969), ranging from 'no vegetation' to 'maximum vegetation'. We then consider the climates at these two extremes, which are approximated by land surface parameters typical for a desert and an evergreen forest, respectively. From an atmospheric standpoint, the desert surface is relatively smooth, shows a higher reflectance (i.e., higher albedo) and has a strongly reduced ability of storing (and consequently recycling) precipitation by evapotranspiration. In contrast, the forest surface is rougher, darker and has a much higher ability of recycling water through evapotranspiration than the desert surface. These two extreme sets of land surface parameters then form the input for two climate model simulations, the ‘desert world’ and the ‘green planet’. The changes are applied to all non-glaciated land regions in a uniform way except for the soil water storage capacity, which is obtained at each individual grid point of the model using an optimisation approach (Kleidon and Heimann, 1998a). By comparing the simulated climates of these two extremes we estimate the maximum effect of vegetation on climate, focusing on the differences in the terrestrial branch of the water cycle and the surface energy balance. Our approach is in fact a continuation of the study by Shukla and Mintz (1982) who used evapotranspiration itself as a proxy of the effect of vegetation on land surface processes. Our approach is an improvement in that the whole range of land surface properties is taken into account. Also, the water balance at the surface remains closed in our approach since we modify parameters rather than processes, thus enabling our approach to yield a more realistic estimate.

What will the implied differences in climate mean to the biosphere? Which are the regions where vegetation will react most sensitively to climate? After inspecting the differences in climate, we use the Köppen climate classification (1923) to assess these questions. As mentioned above, this classification is based on the assumption that the distribution of natural vegetation is a manifestation of climate and its seasonality. Köppen then associated vegetation type boundaries to climatic criteria based on the mean annual and monthly mean extremes of temperature and precipitation. Rather than using this classification for estimating vegetation characteristics and successively determine the equilibrium state of the climate-vegetation system (as in Claussen, 1994), we merely use it to illustrate the differences in the climatic type. If the same climatic type is predicted under both extremes for a particular region, then this would imply that the climate-vegetation system is relatively stable because the same vegetation type is predicted under both extremes. If, however, the outcome is different, this would indicate that the regional vegetation-climate system is sensitive to atmosphere-biosphere interactions, with potential barriers for recovery to the equilibrium state. This analysis also allows us to obtain a first impression on the persistence of the extremes, that is, in which regions the ‘green planet’ (or the ‘desert world’) would maintain itself.

In the next section, we give a brief overview of the formulation of the land surface scheme of the climate model and describe the design of the simulations in more detail. The differences in the simulated climates are presented in Section 3, where the focus is on the global and regional aspects of the hydrological cycle and the surface energy balance. The differences are explained by the underlying mechanisms. Section 4 addresses the issue about the importance of the differences in extreme climates to the vegetation. Implications, ideas about future work and limitations of the results are discussed in Section 5. We close with a summary and conclusion in Section 6.

2. Methods

We use the ECHAM 4 General Circulation Model (Roeckner et al., 1996) in T42 resolution (equivalent to roughly 2.8° lat. $*$ 2.8° long.). The model simulates the general circulation of the atmosphere as well as processes in the atmosphere such as generation of precipitation and cloud formation. The vertical is represented by 19 layers and the computations are performed with a time step of 24 minutes. The model is able to realistically simulate the present day climate (Gates et al., 1999). The control simulation (i.e., the simulation of the present day climate) and the comparison to observations is described e.g., by Wild et al. (1996), Roeckner et al. (1996) and Stendel and Roeckner (1998). An integral part of the model is the land surface. In the following we give an overview of the formulations used to describe the processes at the land surface and explain the setup of the simulations.

2.1. DESCRIPTION OF THE LAND SURFACE PARAMETRISATION

The purpose of the land surface parametrisation within the GCM is to compute the exchange fluxes of heat, water, and momentum between the surface and the atmosphere. Therefore, it simulates the energy and water balance (including snow cover) at the surface and diffusion of heat within the soil using the computed weather of the GCM.

Soil hydrology is calculated by a budget equation. It includes a sophisticated computation of surface runoff (Dümenil and Todini, 1992), which accounts for sub-grid scale heterogeneity of the terrain height. Also, an explicit formulation for slow and fast drainage is used, depending on the water content of the rooting zone. Total evapotranspiration over land has four components: evaporation from snow, from the skin reservoir (i.e., re-evaporation of intercepted water from the canopy), from bare soil, and from transpiration. Transpiration occurs from the vegetated part of the grid cell, which is not covered by snow and where no water can evaporate from the skin reservoir of the canopy. It is determined by the bulk formula approach, a simple formulation of stomatal conductance (based on Sellers et al., 1986) and water stress, obtained from relative soil moisture. The albedo of the surface is calculated from the background albedo (i.e., the albedo of the surface in the absence of snow) and the snow cover.

The land surface of the model is characterised by a set of surface parameters consisting of background albedo, fraction of vegetation cover, leaf area index (LAI), total roughness length (i.e., the composite of both, roughness from orography and vegetation cover), forest fraction, a heterogeneity parameter for runoff computation and soil water storage capacity. The standard set of land surface parameters and its derivation from observations is described by Claussen et al. (1994).

Vegetation affects the land surface parameters in the following way:

- *Background albedo* is generally reduced in the presence of vegetation which then affects the amount of absorbed solar radiation. This effect is reduced when snow covers the surface.
- *Forest ratio* is a pure vegetation parameter describing the fraction of forest coverage. In the presence of forest, the albedo of a snow covered surface is reduced.
- *Leaf area index* is a pure vegetation parameter. It affects the size of the interception storage of rain water in the canopy and the integrated stomatal conductance of the canopy.
- *Vegetation cover* is a pure vegetation parameter. It determines the fraction of the grid cell at which transpiration can occur and thus the relative importance of transpiration to bare soil evaporation.
- *Roughness length* is increased in the presence of vegetation. A rougher surface is generally associated with more efficient transfer of turbulent fluxes of heat, water and momentum.
- *Soil water storage capacity* is increased in the presence of vegetation, mainly through the ability of developing a root system. It determines the storage capacity of water in the soil which is available for evapotranspiration. It is primarily important for evapotranspiration during dry periods.

2.2. SETUP OF THE SIMULATIONS

As outlined in the introduction, we conduct two model simulations in order to investigate the maximum effect of vegetation on climate:

In the '*green planet*' simulation, we set the albedo to 12%, the roughness length of the vegetation to 2 m, the fraction of vegetation and the forest ratio to 100% and the leaf area index to 10. Soil water storage capacities (SWCs) are obtained by an optimisation approach (Kleidon and Heimann, 1998a,b). In this approach, the degree of adaptation of the vegetation (or fitness) is measured by its productivity which is then maximised in order to obtain optimised SWCs. In contrast to the study by Kleidon and Heimann, we use an offline version of the land surface model in order to conduct the optimisation more time efficiently. The distribution obtained from the optimisation is used to compute a new climate and the optimisation is performed again. Two iterations are performed to achieve an equilibrium between the computed, optimised distribution of SWCs and the simulated climate. This methodology effectively results in SWCs that are large enough to ensure maximum soil water availability during dry periods. In addition, we modify the land surface scheme by not allowing for soil drainage, and for surface runoff only in the case when the rooting zone of the soil is at field capacity. The motivation for this is to incorporate a maximum capability of the vegetation to hold water in the soil which is achieved, for instance, by deep roots and by a high infiltration rate due to a high organic content of the soil and biogenic activity/macropores of the soil.

In the '*desert world*' simulation, we set the land surface parameters to desert values: albedo to 28% or higher (if the albedo is higher in the standard set of land surface parameters), roughness length to its orographic values, fraction of vegetation cover and forest fraction to zero, leaf area index to zero and the soil depth to 0.10 m. In order to translate the soil depth to soil water storage capacities, we use the global data set of plant available water of Batjes (1996).

Both of these changes are applied to non-glaciated land regions only. The setup of the simulations is summarised in Table I. Both simulations run for 10 years with the first year discarded in order to exclude spin-up effects. Sea surface temperatures are prescribed to their climatological values. The significance of the changes in climate is estimated by a student's t-test (using a value of $p \leq 0.05$). In the analysis of the results we focus on annual and seasonal (December to February, DJF, and June to August, JJA) means.

3. Difference in Climatic Variables: Green Planet – Desert World

In this section we present the differences between the two simulations in the water cycle and the energy balance at the surface. We first quantify the maximum effect of vegetation in terms of annual means of certain atmospheric variables, averaged over all land regions and over the whole globe. In the second part, we investigate the seasonal and regional aspects in more detail. This section closes with a brief summary of the mechanism and feedback processes. We report the differences as 'green planet' minus 'desert world', that is, as the effect of maximum vegetation.

3.1. GLOBAL DIFFERENCES

Table II shows annual means of atmospheric variables describing the water cycle and the surface energy balance. These means are averages taken over all land points ('land', including the glaciated regions) and over the whole globe ('global', including the oceans). The global balances are not exactly closed because of rounding errors and because of a slight numerical loss of water in the model atmosphere.

We first investigate the differences over land. The hydrological cycle is more active, with precipitation roughly increasing by 100%, evapotranspiration by more than 200% and the mean moisture content of the atmosphere (or precipitable water) increasing by 30%. These increases can be understood by enhanced recycling of soil water as a response of both, (i) more absorbed radiation at the surface so that more energy is available for evapotranspiration and (ii) larger soil water storage capacities (SWCs) which enhance water availability during dry periods. This increased recycling also leads to an overall decrease in continental runoff by about 25%.

TABLE I

Definition of the 'green planet' and 'desert world' experiments

Land surface parameters	Green planet	Desert world	Effect on land surface processes
Background albedo	0.12	0.28	Absorbed solar radiation
Rooting/soil depth	Optimised	0.10 m	Evapotranspiration through storage size of soil water
Roughness length (vegetation)	2 m	0.01 m	Turbulent fluxes of heat, water, and momentum
Leaf area index	10	0	Evaporation through interception storage size, evapotranspiration through stomatal conductance
Vegetation cover	100%	0%	Transpiration
Forest ratio	100%	0%	Absorbed solar radiation through albedo of snow covered surfaces
Land surface processes	**Green planet**	**Desert world**	
Drainage	None	Standard (depending on relative soil moisture)	
Surface runoff	Restricted (only when soil moisture is at field capacity)	Standard (depending on soil moisture and topography)	

The substantial increase in evapotranspiration is associated with differences in the surface energy balance, primarily concerning the partitioning between sensible and latent heat. The latent heat flux increases by the same amount (more than 200%) as evapotranspiration and the sensible heat flux decreases to 30% of its original value. Thus, the Bowen ratio of land regions (calculated from the means) reduces from 1.25 to 0.12 which makes the land surface appear almost like an ocean surface. Subsequently, the increased latent heat flux leads to more efficient

TABLE II

Climatic mean variables of the water budget and the surface energy balance

Annual means	'Desert world'		'Green planet'	
	Land	Global	Land	Global
Water cycle				
Precipitation (in 10^{12} m^3 year^{-1})	71	492	137	547
Evapotranspiration (in 10^{12} m^3 year^{-1})	31	495	108	550
Runoff (in 10^{12} m^3 year^{-1})	37	–	28	–
Precipitable water (in kg m^{-2})	16	23	21	26
Surface energy balance				
Solar net radiation (in W m^{-2})	125	148	130	147
Thermal net radiation (in W m^2)	–75	–57	–52	–49
Sensible heat flux (in W m^{-2})	–23	–13	–8	–9
Latent heat flux (in W m^{-2})	–18	–78	–62	–87
2 m Air temperature (in °C)	9.1	14.6	7.9	14.3
Cloud cover (in %)	50.5	58.7	58.4	60.6

cooling of the surface, resulting in temperatures reduced by 1.2 K. The amount of absorbed solar radiation increases only slightly by less than 5% which is far less than what would be expected from considering the albedo change alone (more than 20%). This difference is the result of greater cloudiness ($\approx +16\%$) in the presence of vegetation (acting as a negative feedback process) attributable to the higher moisture content of the atmosphere due to the increased recycling. The net longwave emission from the surface is reduced by about 30%. The total amount of available energy at the surface thus increases by 26.7 W m^{-2}, with three quarters of this increase attributable to the reduction of net longwave emission.

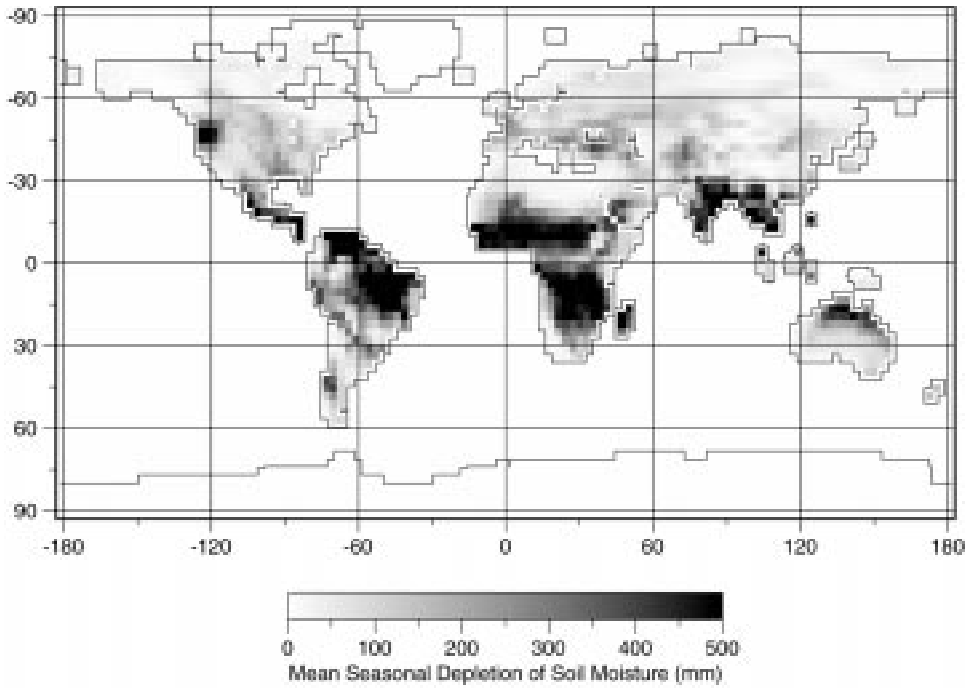

Figure 1. Mean seasonal depletion of soil water in the 'green planet' simulation. Since the storage capacity of plant-available soil water is negligible in the 'desert world' simulation, this figure corresponds roughly to the difference in seasonal soil water depletion.

In terms of global means (including ocean surfaces), the relative changes are naturally smaller. Nevertheless, atmospheric moisture increases by 10% and the heat fluxes at the surface differ in the order of 5 W m^{-2}, with the sensible heat flux being less by 5 W m^{-2} and the latent heat flux greater by 9 W m^{-2} in the presence of maximum vegetation. It is also interesting to note that both precipitation and evapotranspiration decrease over the oceans (11 and 21 10^{12} m^3 $year^{-1}$ respectively). This can be understood in terms of the increased cloudiness by about +4%, reducing the incoming solar radiation at the surface and a modified atmospheric circulation.

3.2. REGIONAL AND SEASONAL DIFFERENCES

In this subsection we show maps of differences in the seasonal means for the northern hemisphere summer/wet season (June–August, JJA, winter/dry season on the southern hemisphere) and southern hemisphere summer/wet season (December–February, DJF, winter/dry season on the northern hemisphere). We start with the differences in the components of the water cycle (Figures 1 and 2), illustrate these differences in terms of annual discharge of major river basins (Figure 3) and end with the differences in the surface energy balance (Figure 4):

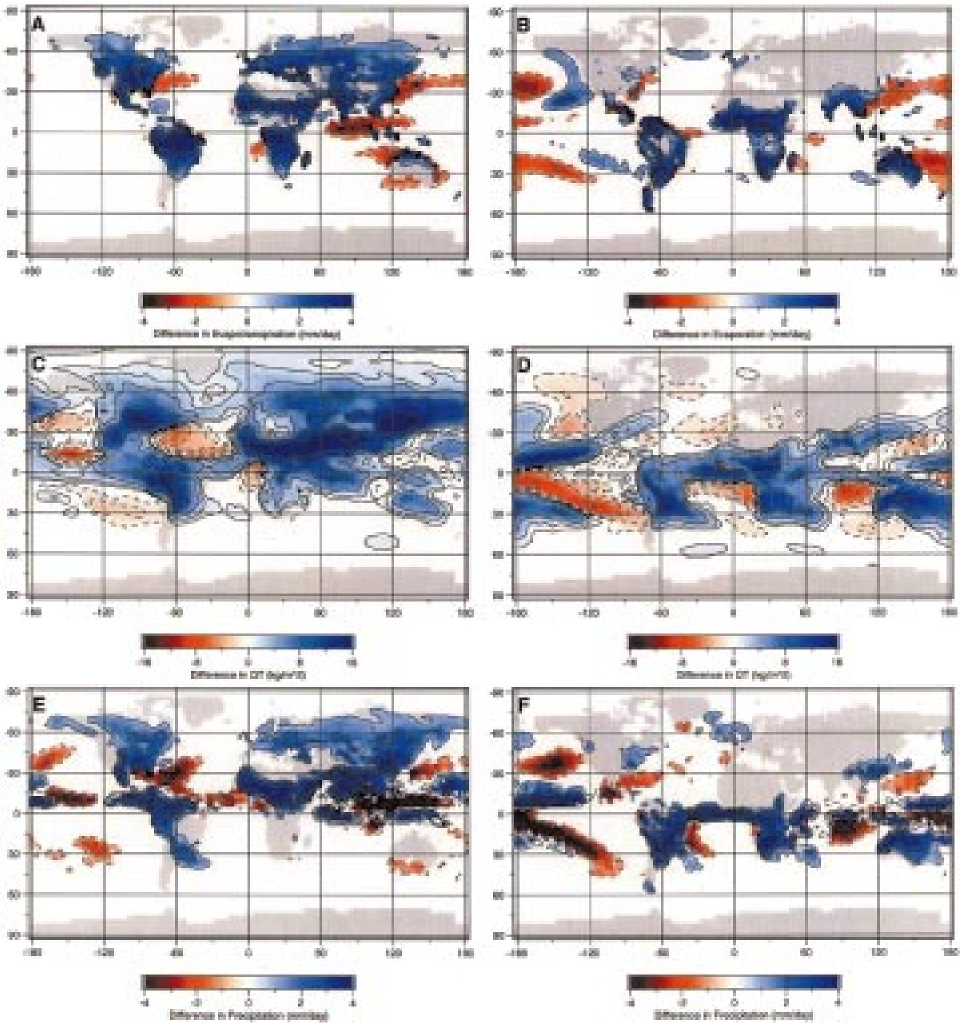

Figure 2. Differences in the water cycle: Seasonal differences between the ‘green planet’ and ‘desert world’ climates for June–August (JJA, left) and December–February (DJF, right). A, B: Evapotranspiration (in mm day^{-1}), C, D: precipitable water (i.e., the vertically integrated moisture content of the atmosphere, ‘QT’, in mm or kg m^{-2}), and E, F precipitation (in mm day^{-1}). Solid (dashed) contour lines denote positive (negative) changes. Contours are at ± 1, 2, 4, 8, 16 mm day^{-1} or mm. Significant changes greater than $\pm$ 1 mm day^{-1} or mm are shown in colour (student’s t-test, $p \leq 0.05$). Zero line contours are omitted. Light grey areas indicate land regions in which no significant changes take place.

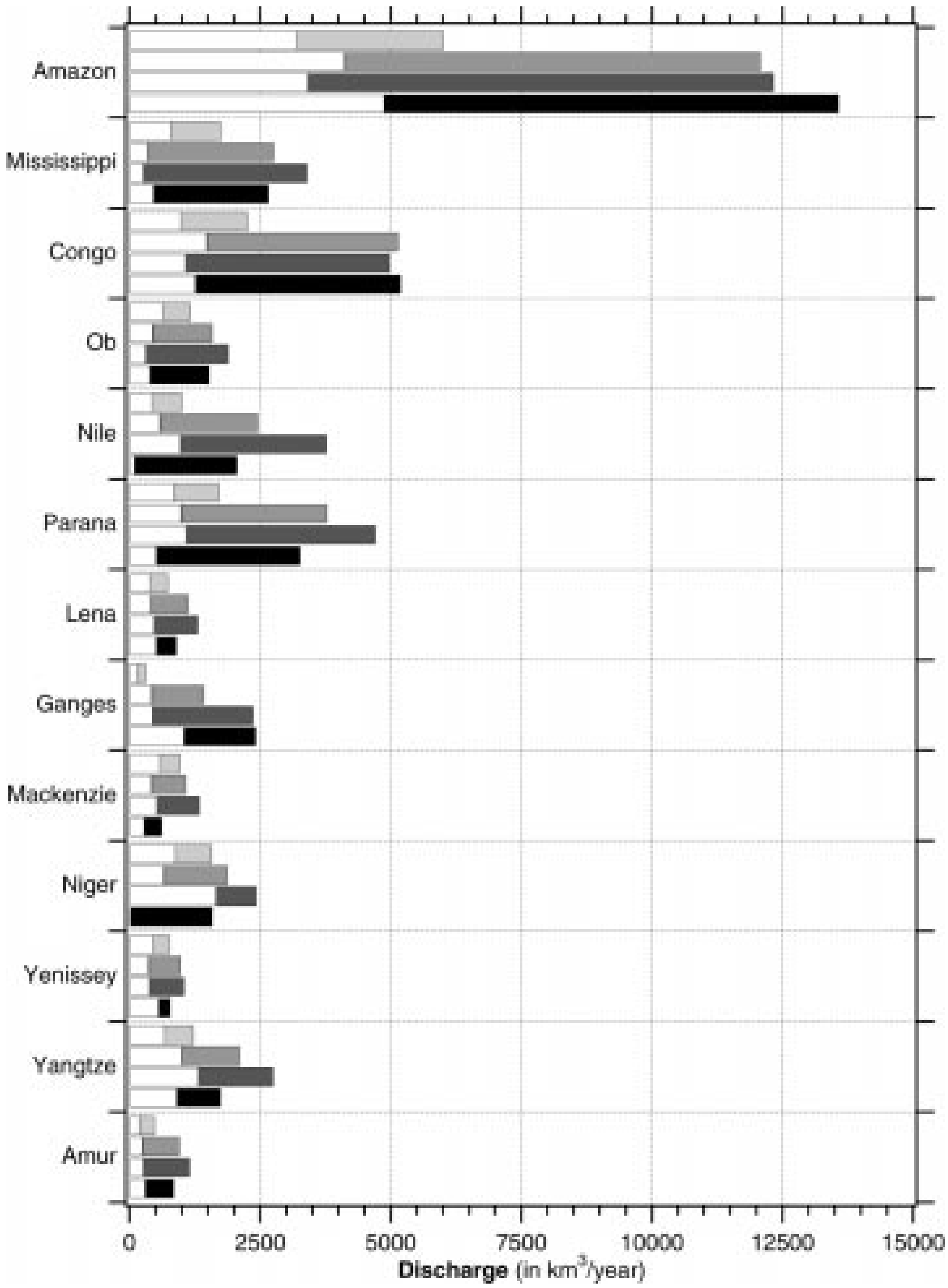

Figure 3. Changes in drainage basin hydrology. Mean annual precipitation and discharge for the world's largest river basins. For each river basin, values are shown for the 'desert world' simulation (top, light grey), the 'control' (medium grey), the 'green planet' (dark grey) and for observations (bottom, black) of precipitation (Legates and Willmott, 1990) and river basin discharge (Dümenil et al., 1993). The longer, coloured bars denote precipitation, the open bars discharge.

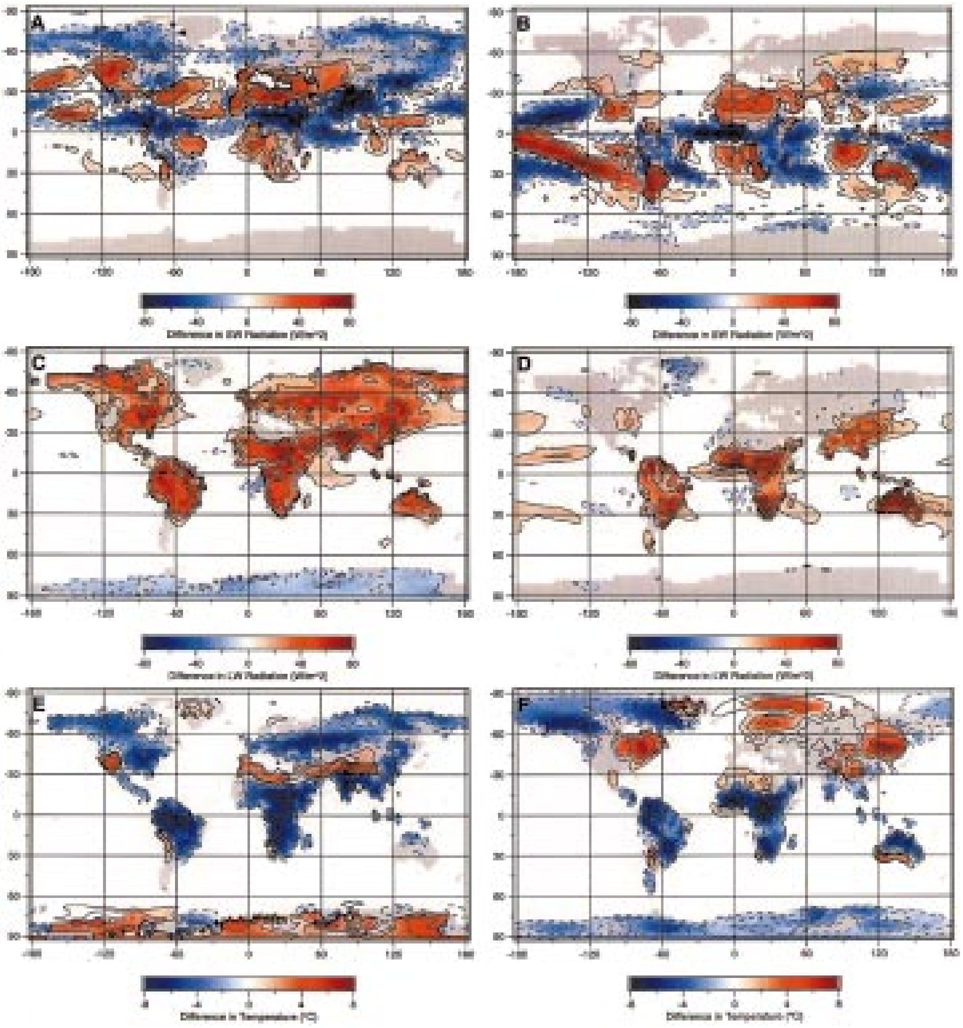

Figure 4. Differences in the surface energy balance: Seasonal differences between the ‘green planet’ and ‘desert world’ climates for June–August (JJA, left) and December–February (DJF, right). A, B: Net solar radiation (in W m^{-2}), C, D: net longwave emission (in W m^{-2}, with positive changes meaning less loss/emission), and E, F: near surface air temperature (in K). Solid (dashed) contour lines denote positive (negative) changes. Contours are at ± 10, 20, 40, 80 W m^{-2} for the radiation plots and ± 1, 2, 4, 8 K for temperature. Significant changes greater than ± 10 W m^{-2} (± 1 K) are shown in colour (student’s t-test, $p \leq 0.05$). Zero line contours are omitted. Light grey areas indicate land regions in which no significant changes take place.

Differences in the water cycle: The presence of maximum vegetation directly affects the surface characteristics and the access to water stored in the soil. Figure 1 shows the seasonal depletion of soil water within the rooting zone in the 'green planet' simulation, which is roughly equivalent to the difference between the two simulations since the soil water storage capacity in the 'desert world' simulation is low. Considerably more water from the soil is recycled in the 'green planet' simulation, with the peaks located in the semiarid tropical regions of Africa, South Asia and South America. This increased depletion is directly linked to enhanced evapotranspiration from these regions during dry seasons. Large scale patterns of increase in evapotranspiration can be found over most continental surfaces (Figures 2a,b). Being in the order of 2–4 mm day^{-1}, they form a substantial increase in evapotranspiration. In temperate regions, these differences are concentrated in the summer months while in most humid tropical regions the differences persist throughout the year. As a result of the substantial increases in evapotranspiration over the continental regions, the atmosphere is moister over most parts of the summer hemisphere and the tropics (Figures 2c,d). A few regions over the ocean show a decrease in atmospheric moisture as a result of differences in the circulation. Precipitation generally increases over continental regions in a similar magnitude as evapotranspiration (Figures 2e,f). Strongest differences are found in the Inter Tropical Convergence Zone (ITCZ), especially over the Monsoonal regions of Southeast Asia/India. In contrast to the persistent increase of evapotranspiration in tropical regions, precipitation mainly increases during the wet season. In temperate regions, precipitation increases during the summer months. The differences in evapotranspiration and precipitation also modify the general hydrology of the land surface. To illustrate how much the hydrology is affected, we integrate the mean annual precipitation (as the input for discharge) and total runoff over the river basins (the difference between precipitation and runoff is equal to evapotranspiration because the water balance is closed on a mean annual basis). Figure 3 shows these integrated values for the 13 largest river basins (by drainage basin size) for the 'green planet' and the 'desert world'. For comparison, we include the values obtained from observations and from the control simulation. Precipitation is more than doubled for most river basins in tropical and subtropical regions (e.g., Amazon, Congo, Nile, Parana, Ganges) while the relative differences are smaller for arctic rivers (e.g., Mackenzie, Yenissey). This is in agreement with the differences shown in Figure 2. River basin discharge is not reduced in all cases in the 'green planet' (e.g., Parana, Niger, Ganges) since the increase in precipitation is larger than the increase in evapotranspiration. It is interesting to note that the transition from the 'desert world' via the 'control' (which can be seen as an intermediate between the extremes) to the 'green planet' does in general not lead to a gradual change in runoff in all river basins (exceptions are, for instance, the Amazon, the Congo and the Niger). This non-uniformity of change can be explained by the different choices for albedo and soil water storage capacity in the control simulation. If, for example, a low surface albedo in the control simulation is not associated with a large soil moisture storage capacity, the climatic response could be different to the 'green planet' simulation in that surface radiation increases, but not necessarily the latent heat flux during dry periods. While this seems to be an artificial effect, it nevertheless points out that some properties (here, river discharge) do not have to be at their extremes in the two extreme simulations (see next section).

Differences in the surface energy balance: The profound differences in evapotranspiration directly affect the surface energy balance through differences in the latent heat flux (proportional to the differences shown in Figures 2a,b, with a conversion factor of approximately 1 mm day^{-1} $\hat{\approx}$ 30 W m^{-2}, which means that the differences in latent heat flux are in the order of 60–120 W m^{-2}). The sensible heat flux (not shown) is reduced by 40–80 W m^{-2} in most regions in which the latent heat flux/evapotranspiration is increased. Areas of increase can also be found, mainly over arid regions where solar radiation increases. Net solar radiation at the surface decreases in the central tropics and humid temperate regions and increases over arid/desert regions (Figures 4a,b). The differences are in the order of 20–40 W m^{-2}. The patterns can be understood as the combined effect of the lower albedo and a modified cloud cover as a response to the increased moisture content of the atmosphere. Cloud cover increases most strongly over the equatorial tropics along the ITCZ and the temperate regions of the northern hemisphere during summer where the increase in cloud cover overcompensates the effect of a lower albedo. A large-scale decrease in net longwave emission in the order of 20–40 W m^{-2} can be found over most continental regions (Figures 4c,d). They are largest in the tropics throughout the year and during summer in the temperate regions. The patterns correspond well with the differences in evapotranspiration (Figures 2a,b). In total, net surface radiation increases in most regions (not shown), mainly as a consequence of the reduced longwave emission from the surface. Large regions show considerably lower air temperatures of up to 8 K (Figures 4e,f) with the largest differences found in the tropics. These patterns are very similar to the regions with increased evapotranspiration (Figures 2a,b). Increases in temperature can also be found, mainly over arid regions. In addition, differences in the temperate and high latitudes occur during winter which can be primarily attributed to changes in the atmospheric circulation (not shown). These indirect effects dominate the differences in the surface climate during northern hemisphere winter. During spring, a large scale warming of up to 6 K occurs in some boreal regions in the northern hemisphere (not shown). Large regions also show a difference in the mean diurnal range of surface temperature (not shown) with similar patterns as in net solar radiation (Figures 4a,b). Regions of decreased net solar radiation generally show a strong reduction in the diurnal range (in the order of 4 K) and regions with increased net solar radiation show a weaker increase (up to 2 K).

3.3. MECHANISM AND FEEDBACK PROCESSES

The effect of maximum vegetation on the global climate can in general be understood by the following mechanism:

In the presence of vegetation, more solar radiation is absorbed due to the lower albedo and more soil water is available for transpiration due to increased access to soil water. Both factors increase evapotranspiration, leading to enhanced cooling of the surface through the associated latent heat flux. More evapotranspiration also enhances the input of moisture into the atmosphere thus to moister air. Other factors, like the increased leaf area index and roughness length, enhance this response: while the increased leaf area favours enhanced interception of rainfall in the canopy (which further enhances the recycling capacity of water), the rougher surface increases the turbulent fluxes. While all these changes contribute to the overall response during wet periods, the large increase in evapotranspiration during dry periods (northern tropics in DJF, Figure 2a, southern tropics and northern temperate in JJA, Figure 2b) can only be attained through the larger access and depletion of soil water (Figure 1).

This mechanism is amplified by positive feedback processes:

– Increased water recycling: enhanced atmospheric moisture favours precipitation which leads to more evapotranspiration in water-limited (arid) regions.
– Increased surface radiation: two processes further enhance the net surface radiation available for the turbulent fluxes of heat, especially evapotranspiration (in radiation limited/humid regions). First and most important, lower surface temperatures lead to a reduced emission of longwave radiation at the surface. Second, more atmospheric moisture reduces the transmissivity of the atmosphere to longwave radiation thus further reducing the net emission of longwave radiation at the surface.

One negative feedback counteracts this mechanism:

– Increased cloud cover: more atmospheric moisture favours more clouds, thus reducing the amount of solar radiation at the surface.

This mechanism affects the local, climatic environment for plants. Lower air temperatures and more atmospheric moisture both lead to a reduced vapour-pressure deficit thus reducing the atmospheric demand for evapotranspiration and consequently water stress. This could be understood as an additional, positive ‘biologic’ feedback process.

4. Implications of the ‘Green Planet’ and the ‘Desert World’ Climates

Given the simulated climates of the two extremes, what would the implications be for the vegetation? In other words, would these differences be large enough to fundamentally change the character of the climate thus favouring other types of vegetation? In this section we assess these questions by using the Köppen climate classification, which is explained in the next paragraph before the results are described and discussed. Regions in which the differences in climate lead to different classifications are especially sensitive to vegetation change. Note that we do not address the question whether the favoured vegetation would sustain, that is, lead to multiple equilibria in the climate-vegetation system (as in Claussen, 1998).

4.1. THE KÖPPEN CLIMATE CLASSIFICATION

We apply the Köppen (1923) classification here in terms of its five major types. Köppen's classification is based on the assumption that the distribution of natural vegetation represents certain climatic characteristics. Köppen then associated climatic conditions with biogeographical boundaries using annual means and monthly extremes of climatic variables. For instance, the tree line in high latitudes is described by the condition that the mean temperature of the warmest month is 10 °C. There are certainly more sophisticated and more plant physiologically based approaches; however, we decided to use this classification because of its simplicity, because it is based solely on mean climatic forcing variables (precipitation and temperature which are easily available from the model simulation in a consistent way) and because it does not make use of any additional, ecologically related assumptions.

The Köppen classification defines climatic types in terms of biogeographical boundaries. These boundaries are associated with mean annual or monthly values of temperature and precipitation as given in Table III (see table caption for definitions). Four of the types are defined by temperature limits (A: tropical, C: temperate, D: cold, E: polar) in connection with a moisture requirement while type B (arid) is only described by its moisture budget. Three of these climates represent forest climates: A (tropical forests, including dry-deciduous forest and savanna), C (temperate forests, including deciduous and evergreen) and D (boreal, or needleleaf evergreen/deciduous). The computation of the Köppen classification from the mean monthly climates is performed as in Lohmann et al. (1993) and WBGU (1998). We compute the mean monthly temperatures from the two model simulations and use the association as given in Table III.

4.2. DISTRIBUTION OF CLIMATIC TYPES

The percentage of global land coverage for each climatic type is shown in Table IV for the 'green planet' and the 'desert world'. About a quarter (22.9%) of the total land area shows a different climatic type. The majority of this difference originates from more regions classified as 'arid' in the 'desert world' while more regions are classified as 'temperate' in the 'green planet'. This shift implies a transition in climatic character from one which would favour grassland or desert to one that would favour a temperate forest.

TABLE III
Classification of main climatic types according to Köppen (1923)

Climatic type	Temperature condition	Moisture condition	Vegetation type
A: tropical	$T_{MIN} \geq 18\,°C$	$P_{AVG} > P_D$	Tropical forest and savanna
B: arid/dry	–	$P_{AVG} \leq P_D$	Grassland and shrubland (desert)
C: temperate	$-3\,°C \leq T_{MIN} \leq 18\,°C$	$P_{AVG} > P_D$	Temperate forest
D: cold/snow	$T_{MIN} \leq -3\,°C$ and $T_{MAX} \geq 10\,°C$	$P_{AVG} > P_D$	Boreal forest
E: ice	$T_{MAX} < 10\,°C$	$P_{AVG} > P_D$	Tundra (ice)

T_{MIN} = mean temperature of the coldest month; T_{MAX} = mean temperature of the warmest month; T_{AVG} = annual mean temperature; P_{AVG} = annual mean precipitation; P_D = dryness threshold, defined (in cm month^{-1}) as $2 * T_{AVG}$ if at least 80% of the annual precipitation occur in winter, $2 * T_{AVG} + 28$ if at least 70% of the annual precipitation occurs in summer and $2 * T_{AVG} + 14$ otherwise, with temperature measured in centigrade (°C).

TABLE IV
Percentage of land cover of Köppen's climatic types

Climatic type	Green planet	Desert world
A: tropical	19.4%	18.1%
B: arid/dry	9.1%	28.2%
C: temperate	29.4%	12.2%
D: cold/snow	23.5%	27.3%
E: ice	18.5%	14.2%

The computed maps of climatic types for the 'green planet' and the 'desert world' are shown in Figure 5. The distribution obtained from the simulation with present-day land surface parameters and as obtained from a global climatology (Cramer and Leemans, pers. comm., updated version of Leemans and Cramer, 1991) are also shown for comparison. Most of the extratropical regions and the central tropics show hardly any differences in the climatic type between the two extreme simulations. This implies that these regions would still favour the existing vegetation type at present despite the strong changes in surface climate (which might lead to a different species distribution). Considerable differences are found in most arid regions, especially large parts of Africa, South/Central Asia and Aus-

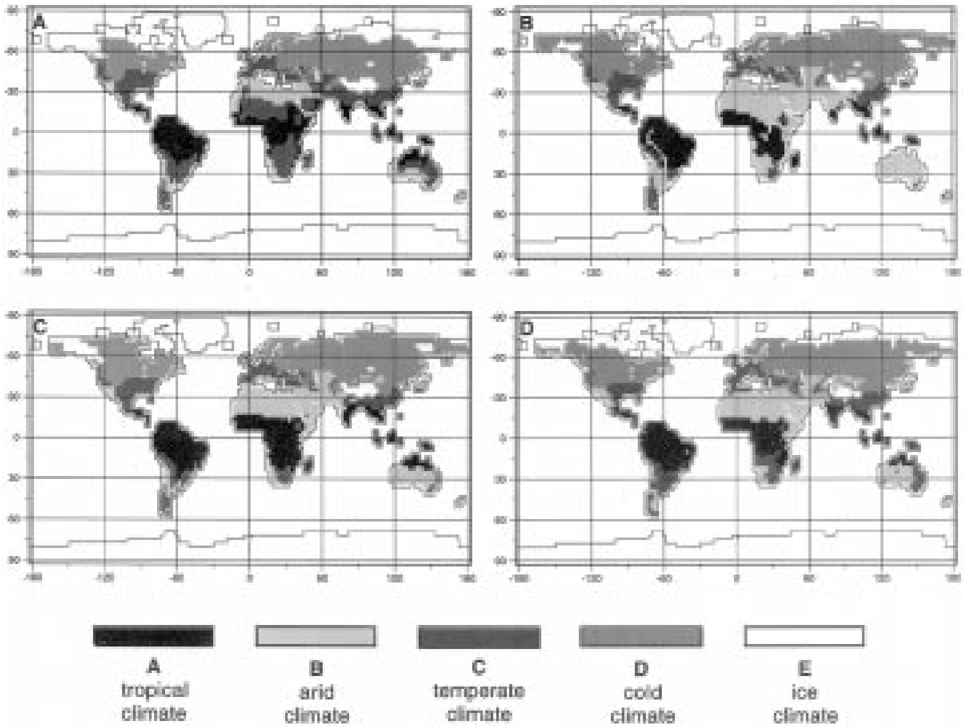

Figure 5. Classification of climates according to Köppen. A: the 'green planet', B: the 'desert world', C: the ECHAM control, and D: the observed climatology of Cramer and Leemans (pers. comm., updated version of Leemans and Cramer, 1991). The regions of largest differences between the 'green planet' and the 'desert world' point out regions in which the climatic differences would affect vegetation most strongly.

tralia. In these regions, large parts are classified as temperate climates in the 'green planet' simulation, implying that the simulated climate would favour a forest. On the other hand, in the 'desert world' simulation these regions are classified as arid climates thus not favouring a forest but rather a grassland or a desert. This difference can be understood by the strong influence of the vegetation on the climate in these regions. This also means that the ecosystems there are potentially too fragile to disturbances (see also discussion below).

5. Discussion

In this section we will first compare the magnitude of the differences with sensitivity studies of other investigators and then discuss the limitations of the approach and the results.

5.1. COMPARISON TO OTHER STUDIES

– *Magnitude and patterns of differences:* The magnitude of the differences between the 'green planet' and the 'desert world' correspond well with other sensitivity studies on isolated land surface aspects influenced by vegetation. For instance, our results conform to the mechanism suggested by Charney (1975) by which an albedo change associated with vegetation change could favour the persistence of a desert in the Sahel. The results presented here are also in general agreement with the sensitivity study by Milly and Dunne (1994) who investigated the sensitivity of the climate system to soil water storage capacity with a series of GCM simulations. Their spatial and temporal patterns of difference in the water cycle correspond well with the ones shown in Figure 2 although the magnitude here is somewhat larger. This can be attributed to the simultaneous change of a series of land surface parameters in our simulations. The spring-time warming over the northern boreal regions agree with the results of Bonan et al. (1992) who showed that the darker surface albedo of snow covers in the presence of forests leads to large-scale warming during spring.
– *Mechanism:* Eltahir (1998) proposed a mechanism by which soil moisture conditions affect the generation of precipitation and demonstrated this mechanism at hand of observations. Our results are in very good agreement with this mechanism (see also Section 3.3), especially the strong feedback through the changes in net longwave radiation on the surface energy balance.
– *Sensitivity of the vegetation-climate system:* Our results are in qualitative agreement with the sensitivity study by Claussen (1998), who investigated the equilibrium of vegetation-atmosphere system using different initial conditions (similar to our 'desert world' and 'green planet' simulations) with a coupled biome-climate model. Claussen found that the equilibrium state of the vegetation-atmosphere system depended on the initial distribution of biome type in the Sahara region and Central Asia and concluded that these regions are most sensitive to changes in vegetation cover. Our results agree with this conclusion. However, we find a much more pronounced response which can be explained by the differences in rooting depth/soil water storage capacity that we considered in our simulations and the resulting intensification in the water cycle. In addition, we find that other arid regions are equally as sensitive, for instance Australia and South Africa. However, our analysis does not allow for conclusions whether these are two distinct stable states.

In summary, we find that the results reported here are in agreement to earlier studies in terms of (i) the magnitude and patterns of earlier sensitivity studies to isolated land surface parameters, (ii) the mechanism causing the differences, and (iii) the pattern of sensitivity of the vegetation-climate system.

5.2. LIMITATIONS

Besides the limitations inherent to the parameterisations used within the model (which we will not discuss here) there are limitations to our approach:

- *Concept of 'maximum vegetation':* This study should be seen as a first attempt in estimating the maximum range at which vegetation has the 'power' to affect the physical climate system. It has been implemented in a crude way in which constraints such as water, carbon/productivity, heat and nutrients have been neglected. These constraints certainly affect the state of the vegetation and thus the development of land surface characteristics such as albedo, leaf area index or rooting depth. In a more sophisticated approach, these constraints could be incorporated to yield a more realistic estimate. However, the estimate given here should remain valid as an upper bound of the maximum effect of vegetation on climate.
- *Maximum effect:* Here, we only considered 'sustainable' effects on climate. For instance, large scale irrigation of land which utilises water not derived from the same region (i.e., grid point) could lead to climatic effects which are not included in this study. The maximum effect may also be overestimated in desert regions, where the dark albedo used in the 'green planet' simulation may not be sustained by the vegetation.
- *'Green Sahara':* While many regions do not show a substantial change in climatic character (despite some changes in temperature and precipitation), particularly strong changes are found in most arid regions, especially in Africa, and are predicted to maintain a substantially 'greener' vegetation state than what is observed. This could be caused by a series of factors which we briefly discuss here:
    - Overestimation of the model's response to vegetation characteristics. This could be investigated by conducting similar simulations with other climate models.
    - Other processes stop the advance of the forest. These processes could be of natural origin, such as oceanic feedbacks (see also below) and disturbances (e.g., fire, climatic variability), of biogenic origin (e.g., grazing) or human influence (land use, grazing). An oceanic response could act as a negative feedback through lower sea surface temperatures and thus supply less moisture to the land regions. The other processes could interrupt the recycling chain from the ocean through the vegetation further landwards making a forest ecosystem too fragile.
    - It could, nevertheless, also be the consequence of two stable states of the vegetation-climate system under present day conditions, as proposed by Claussen (1998).
- *Oceanic feedbacks:* Both simulations were performed with prescribed, climatological sea surface temperatures which do not allow for oceanic feedbacks.

However, the differences over the ocean as shown in Figures 2 and 4 suggest that the remote effect of vegetation is considerable, in particular over the western boundary currents in the northern mid-latitudes. These could lead to subsequent changes in the oceans, for instance in the sea-surface temperature and the meridional heat transport. Also, the study by Bonan et al. (1992) suggests, that sea-ice feedbacks could take place, that is, that the springtime warming over the boreal regions could lead to less sea-ice which would amplify the warming. However, the simulations conducted here do not allow to assess the question whether these changes would act as a positive feedback, thus enhancing the global sensitivity to vegetation change, or would act to compensate the overall response. One might speculate that if oceanic and sea-ice feedbacks were allowed for, the overall effect of vegetation would be a thermostat effect, that is, cooler tropics and a warmer arctic.

6. Conclusion

In this study we investigated the question to which extent vegetation can affect climate. This was done by a new approach where we used the benefits of coupled biome-climate models (which emphasise the fact that land surface parameters should not be treated as independent parameters since they represent different aspects of vegetation) and combined it with two climate model simulations at the extreme stages of ecological succession. By comparing the two extreme climates, we were then able to obtain an estimate for the maximum effect of vegetation on the land surface climate and the global water cycle. Most of the climatic effects could be understood by the differences in continental evapotranspiration, which subsequently affect the surface energy balance and the atmosphere. The climatic effects are considerable, but by employing the Köppen biogeography model we estimated that they would mainly affect the biome types in semiarid regions of the present-day climate. In summary, this study sets an upper limit to the maximum range of the coupled vegetation-climate system.

Three related aspects seem worth to be further investigated in the future: firstly, it would be intriguing to find out how much the isolated effects of parameter changes contribute to the total response. We may speculate that the albedo effect plays a dominant role during the wet season (since water storage is of minor importance during this period), while the rooting depth effect is more important during the dry season. However, ultimately all these parameters are interconnected since vegetation will, for example, not stay green (and dark in terms of albedo) in the absence of sufficient water (which may be explored by a deep root system), a possible reason for the reduced stability of a ‘Green Sahara’. This may nevertheless give insight about the general evolution and interrelationships of these land surface parameters with climate. Secondly, it is interesting to find out in which regions oceanic feedbacks would intensify or reduce the response. Thirdly, a prominent question is how the greenhouse effect of the vegetation (which may be altered by land use change) compares to the anthropogenic greenhouse effect and how both are influenced by each other.

Acknowledgements

The computations were performed at the German Climate Computing Centre (DKRZ). We thank Ulrike Lohmann who implemented the Köppen scheme and provided the program to us, and Stefan Hagemann and the Global Runoff Data Centre for providing the river basin discharge data. This study contributes to the 1999 Report of the Scientific Advisory Board on the Global Environment (WBGU) to the German Federal Government. The simulated climates are available upon request from Axel Kleidon (akleidon@leland.stanford.edu).

References

Batjes, N. H.: 1996, 'Development of a World Data Set of Soil Water Retention Properties Using Pedotransfer Rules, *Geoderma* **71**, 31–52.

Bonan, G. B., Pollard D., and Thompson S. L.: 1992, 'Effects of Boreal Forest Vegetation on Global Climate', *Nature* **359**, 716–718.

Budyko, M. I.: 1974, *Climate and Life*, Academic Press, New York, p. 508.

Charney, J. G.: 1975, 'Dynamics of Deserts and Drought in the Sahel', *Quart. J. Roy. Meteorol. Soc.* **101**, 193–202.

Claussen, M.: 1994, 'On Coupling Global Biome Models with Climate Models', *Clim. Res.* **4**, 203–221.

Claussen, M., Lohmann U., Roeckner E., and Schulzweida, U.: 1994, 'A Global Data Set of Land Surface Parameters', Report 135, Max-Planck-Institut für Meteorologie, Hamburg.

Claussen, M.: 1998, 'On Multiple Solutions of the Atmosphere-Vegetation System in Present-Day Climate', *Global Change Biol.* **4**, 549–559.

Dümenil, L. and Todini E.: 1992, 'A Rainfall-Runoff Scheme for Use in the Hamburg Climate Model', in Kane, J. (ed.), *Advances in Theoretical Hydrology – a Tribute to James Dooge*, Elseviers Science Publishers, Amsterdam, pp. 129–157.

Eltahir, E. A. B.: 1998. 'A Soil Moisture-Rainfall Feedback Mechanism. 1. Theory and Observations', *Water Resour. Res.* **34**, 765–776.

Foley, J. A., Prentice, I. C., Ramankutty, N., Levis, S., Pollard, D., Sitch, S., and Haxeltine, A.: 1996, 'An Integrated Biosphere Model of Land Surface Processes, Terrestrial Carbon Balance, and Vegetation Dynamics', *Global Biogeochem. Cycles* **10**, 603–628.

Gates, W. L., Boyle, J. S., Covey, C., Dease, C. G., Doutriaux, C. M., Drach, R. S., Fiorino, M., Glecker, P. J., Hnilo, J. J., Marlais, S. M., Phillips, T. J., Potter, G. L., Santer, B. D., Sperber, K. R., Taylor, K. E., and Williams, D. N.: 1999, 'An Overview of the Results of the Atmospheric Model Intercomparison Project (AMIP I)', *Bull. Amer. Meteorol. Soc.* **80**, 29–56.

Gutman, G., Ohring, G., and Joseph, J. H.: 1984, 'Interaction between the Geobotanic State and Climate: A Suggested Approach and a Test with a Zonal Model', *J. Atmos. Sci.* **41**, 2663–2678.

Henderson-Sellers, A.: 1993. 'Continental Vegetation as a Dynamic Component of a Global Climate Model: A Preliminary Assessment', *Clim. Change* **23**, 337–377.

Holdridge, L. R.: 1947, 'Determination of World Plant Formations from Simple Climatic Data', *Science* **105**, 367–368.

Kleidon, A. and Heimann M.: 1998a, 'A Method of Determining Rooting Depth from a Terrestrial Biosphere Model and Its Impacts on the Global Water- and Carbon Cycle', *Global Change Biol.* **4**, 275–286.

Kleidon, A. and Heimann M.: 1998b, 'Optimised Rooting Depth and its Impacts on the Simulated Climate of an Atmospheric General Circulation Model', *Geophys. Res. Lett.* **25**, 345–348.

Köppen, W.: 1923, *Die Klimate der Erde*, Walter de Gruyter, Berlin.

Leemans, R. and Cramer, W.: 1991, 'The IIASA Climate Database for Mean Monthly Values of Temperature, Precipitation and Cloudiness on a Terrestrial Grid', RR-91-18, Institute of Applied Systems Analysis, Laxenburg/Austria.

Lohmann, U., Sausen, R., Bengtsson, L., Cubasch, U., Perlwitz, J., and Roeckner, E.: 1993, 'The Köppen Climate Classification as a Diagnostic Tool for General Circulation Models. *Clim. Res.* **3**, 177–193.

Milly, P. C. D. and Dunne K. A.: 1994, 'Sensitivity of the Global Water Cycle to the Water-Holding Capacity of Land', *J. Clim.* **7**, 506–526.

Odum, E. P.: 1969, 'The Strategy of Ecosystem Development', *Science* **164**, 262–270.

Pielke, R. A., Avissar, R., Raupach, M., Dolman, A. J., Zeng, Y., and Denning, S.: 1998, 'Interactions Between the Atmosphere and Terrestrial Ecosystems: Influence on Weather and Climate', *Global Change Biol.* **4**, 461–475.

Prentice, I. C., Cramer, W., Harrison, S., Leemans, R., Monserud, R. A., and Solomon, A. M.: 1992. 'A Global Biome Model Based on Plant Physiology and Dominance, Soil Properties and Climate', *J. Biogeogr.* **19**, 117–134.

Roeckner, E., Arpe, K., Bengtsson, L., Christoph, M., Claussen, M., Dümenil, L., Esch, M., Giorgetta, M., Schlese, U., and Schulzweida, U.: 1996, 'The Atmospheric General Circulation Model ECHAM-4: Model Description and Simulation of Present-Day Climate', Report 218, Max-Planck-Institut für Meteorologie, Hamburg.

Schlesinger, W. H.: 1997, *Biogeochemistry. An Analysis of Global Change*, Academic Press, San Diego, p. 588.

Sellers, P. J., Mintz, Y., Sud, Y. C., and Dalcher, A.: 1986, 'A Simple Biosphere Model (Sib) for Use within General Circulation Models', *J. Atmos. Sci.* **43**, 505–531.

Shukla, J. and Mintz, Y.: 1982, 'The Influence of Land-Surface-Evapotranspiration on the Earth's Climate', *Science* **247**, 1322–1325.

Stendel, M. and Roeckner, E.: 1998, 'Impacts of Horizontal Resolution on Simulated Climate Statistics in ECHAM 4', Report 253, Max-Planck-Institut für Meteorologie, Hamburg.

Vitousek, P. M., Mooney, H. A., Lubchenco, J., and Melillo, J. M.: 1997, 'Human Domination of Earth's Ecosystems', *Science* **277**, 494–499.

WBGU: 1998, *World in Transition: Ways Towards Sustainable Management of Freshwater Resources*, German Advisory Council on Global Change (WBGU), Springer Verlag, Berlin.

Wild, M., Ohmura, A., Gilgen, H., Roeckner, E., and Giorgetta, M.: 1996, 'Improved Representation of Surface and Atmospheric Radiation Budgets in the ECHAM4 General Circulation Model', Report 200, Max-Planck-Institut für Meteorologie, Hamburg.

(Received 13 October 1998; in revised form 23 April 1999)